Self-commissioning calculation of dynamic models for synchronous machines with magnetic saturation using flux as state variable

Riccardo Antonello[1], Luca Peretti[2] ✉, Fabio Tinazzi[3], Mauro Zigliotto[3]

[1]*Dept. of Information Engineering, University of Padova, Italy*
[2]*Department of Electric Power and Energy Systems, KTH Royal Institute of Technology, Stockholm, Sweden*
[3]*Dept. of Management and Engineering, University of Padova, Italy*
✉ *E-mail: lucap@kth.se*

Abstract: This paper deals with the non-linear modelling of synchronous machines by using the flux linkage as a state variable. The model is inferred from a conventional set of measurements where the relation between the currents and the flux linkages in the rotating reference frame (also known as dq reference frame) are known by measurements or estimated through finite-element simulations. In particular, the contribution of this paper is twofold: first, it proposes a method to extract the non-linear model information which can be easily implemented in electric drives, without the need of offline post-processing of the data. Second, it mathematically demonstrates that the method converges to the final result in a stable way. An example based on experimental measurements of the current-to-flux look-up tables of an 11-kW synchronous reluctance machine is shown, proving the feasibility of the proposed method.

1 Introduction

In modern electric drives, digital modelling of electric machines play an essential role in the regulation of torque and speed. Precise, dynamically fast and robust (against parameter variation) regulation requires models which are more than just linear. Moreover, as the drives technology develops and more sophisticated solutions for position- and speed-sensorless control are implemented, the use of non-linear models to accurately reproduce the machine behaviour may be required, if not for the control algorithm itself, at least to prove the stability of robust control structures in suitable simulations [1].

As a matter of fact, electric machines are very non-linear devices. The most evident non-linearity is the magnetic saturation, which does not allow to describe the relation between currents and flux linkages with just a simple proportional gain (the inductance) [2]. In the case of synchronous machines, and depending on the design, the magnetic saturation is sometimes accompanied by the magnetic cross-saturation, where the direct-axis flux linkage is influenced by the quadrature-axis current and vice versa [3, 4]. Other important non-linear effects relate to slot effects [5], iron losses [6], and the variation induced by temperature changes of stator/rotor resistances [7], and flux linkages due to magnets [8].

Focusing on magnetic saturation with cross-saturation in synchronous machines, it is known that such effects can be either estimated with finite element analysis or measured with experimental tests, typically during the commissioning stage of an electric drive [9]. Such information usually comes in the form of flux linkages as function of currents, typically in the *dq* reference frame. However, the inclusion of such non-linear information in digital models is not straightforward, because it depends on whether the *dq* currents or the *dq* flux linkages are used as the state variables.

In this perspective, very limited scientific material focuses on methodologies that allow for a description of the magnetic saturation with cross-saturation effects when the flux linkage is the state variable, in all digital models where such choice is made. One of such works is [10], where a polynomial approximation approach is used. However, the problem of calculating the reverse saturation function (from flux linkages to stator currents) from the simulated or measured saturation curves is only partially explored in its nature. Therefore, this work proposes some further steps towards the implementation and commissioning of synchronous machine models with the flux linkage as the state variable, by:

- Proposing a method to obtain the reverse magnetic saturation functions, by means of a scheme that can be easily implemented and executed in any drive control board.
- Demonstrating the stability of the method and the conditions for its convergence.

The paper is organised as follows: Section 2 recalls the basics of synchronous machine modelling, while Section 3 describes the proposed method to extract the non-linear inverse saturation curves, from a set of saturation curves which return the flux linkages as function of currents. Section 4 analyses the convergence of the method, proving its stability. Section 5 demonstrates the use of the method on the saturation curves of 11-kW synchronous reluctance machine (SynRM), followed by some final remarks in the conclusions.

2 Synchronous machine model theory

There are essentially two ways to model synchronous machines, shown in (1) in their space-vector equation form in a *dq* reference frame synchronous to the rotor:

$$\frac{di_{sdq}}{dt} = L^{-1}(u_{sdq} - R_s i_{sdq} - J\omega_{me}\lambda_{sdq})$$

$$\frac{d\lambda_{sdq}}{dt} = u_{sdq} - R_s i_{sdq} - J\omega_{me}\lambda_{sdq}$$

(1)

where u, i, λ are the space vectors of stator voltages, currents and flux linkages, respectively. L is the incremental inductance matrix and J accounts for the *dq*-axes cross-coupling:

$$\boldsymbol{L} = \begin{bmatrix} L_{dd} & L_{dq} \\ L_{qd} & L_{qq} \end{bmatrix} = \begin{bmatrix} \dfrac{\partial \lambda_{sd}}{\partial i_{sd}} & \dfrac{\partial \lambda_{sd}}{\partial i_{sq}} \\ \dfrac{\partial \lambda_{sq}}{\partial i_{sd}} & \dfrac{\partial \lambda_{sq}}{\partial i_{sq}} \end{bmatrix}, \quad \boldsymbol{J} = \begin{bmatrix} 0 & 1 \\ 1 & 0 \end{bmatrix} \quad (2)$$

It is worth to recall that the conservation of energy principle implies the reciprocity condition in (2), hereafter expressed on the left for the currents as state variables (upper equation in (1)) and on the right for the flux linkages as state variables (lower equation in (1)):

$$\frac{\partial \lambda_{sd}}{\partial i_{sq}} = \frac{\partial \lambda_{sq}}{\partial i_{sd}} \quad \frac{\partial i_{sd}}{\partial \lambda_{sq}} = \frac{\partial i_{sq}}{\partial \lambda_{sd}} \quad (3)$$

The iron losses are excluded, since this work focuses on the relation between flux linkages and currents. Anyway, more accurate models including iron losses are available in literature, for example in [6, 11, 12].

The model with the stator currents as state variables implies the calculation of the incremental inductances $\boldsymbol{L}$, defined as derivatives of the flux linkage with respect to the currents. Consequently, the use of stator flux linkages for real-time modelling purposes (for example, in full-order observers where the flux estimation is available) is to be preferred, since simpler equations are obtained [10]. The related block schematic is reported in Fig. 1.

The drawback of such formulation is that the magnetic saturation has to be modelled in the form $i_{sdq} = \boldsymbol{f}_{dq}^{-1}(\lambda_{sdq})$, where $\boldsymbol{f}_{dq}$ is the function relating the stator currents to the flux linkages:

$$\lambda_{sdq} = \boldsymbol{f}_{dq}(i_{sdq}) = \begin{bmatrix} \lambda_{sd}(i_{sd}, i_{sq}) \\ \lambda_{sq}(i_{sd}, i_{sq}) \end{bmatrix} \quad (4)$$

It is worth to note that the flux linkage is a typical result of self-commissioning identification procedures of synchronous machines, in the form of two bi-dimensional look-up tables (LUTs). Solutions that generate LUTs are available in the literature, as for example [9] for the case of synchronous reluctance machines.

3 Proposed method

Once stored, the LUTs describing $\boldsymbol{f}_{dq}$ can be used to determine the inverse function $\boldsymbol{f}_{dq}^{-1}$ by means of the schematic shown in Fig. 2, which is an easily-implementable loop algorithm running within the drive control board for each selected flux reference. In the block diagram, C represents a suitable MIMO (i.e. two-inputs, two-outputs) controller that is designed to stabilise the feedback loop, and to guarantee the regulation of the output λ_{sdq} to the specified set-point λ_{sdq}^* with a satisfactory settling (i.e. convergence) time. Each point of the flux-to-currents LUTs describing the inverse map $i_{sdq} = \boldsymbol{f}_{dq}^{-1}(\lambda_{sdq})$ is obtained by setting an appropriate value of the flux linkage reference vector λ_{sdq}^*, and then evaluating the value of the current vector i_{sdq} achieved at steady state (such value certainly exists, provided that C is a stabilising controller that guarantees zero steady-state regulation error). Obviously, the resolution of the LUTs so obtained is in trade-off with the memory consumption and the computing time of the control board microprocessor/FPGA.

The next section shows that a pure integral controller is sufficient to guarantee stability and perfect regulation of the flux linkage. An upper bound to the convergence time is also derived, which can be used next as a design constraint for the controller gain.

4 Convergence analysis

This section is devoted to the convergence analysis of the proposed method. A sufficient condition (*inverse function theorem*) for the local invertibility of the function f_{dq}, assumed to be sufficiently smooth (at least continuously differentiable) over a compact set D, is that the Jacobian matrix $\boldsymbol{L} = \partial \boldsymbol{f}_{dq}/\partial i_{sdq}$ is not zero on D, namely

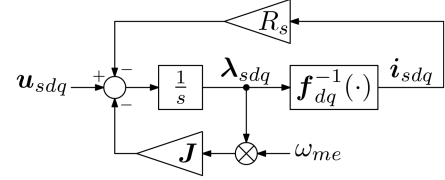**Fig. 1** *Machine model with flux linkage as state variable*
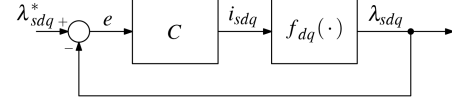

Fig. 2 *Simplified schematic of the proposed method for the determination of the inverse magnetic saturation map*

$$\det \boldsymbol{L}(i_{sdq}) \neq 0 \quad \forall i_{sdq} \in D \quad (5)$$

This condition is certainly verified for any $i_{sdq} \neq \boldsymbol{0}$, since $\boldsymbol{L}$ is a positive definite matrix (as a matter of fact, $(1 = 2)\, i_{sdq}^T \boldsymbol{L} i_{sdq}$ is the stored magnetic energy, which is a positive definite function [13]).

Consider a pure integral controller of the type:

$$\frac{\mathrm{d}i_{sdq}}{\mathrm{d}t} = ke \quad \text{with} \quad k > 0 \quad (6)$$

Thanks to the positive definiteness of the inductance matrix $\boldsymbol{L}$, it is possible to show that there always exists a suitable choice of the integral gain k that stabilises the feedback loop, with a prescribed upper-bound to the settling time. For such purpose, consider the quadratic, positive-definite function:

$$V(e) = e^T e = \| e \|^2 \quad (7)$$

Such function is a valid Lyapunov function that can be used to prove the asymptotic stability of the closed loop, provided that its time derivative $\dot{V}(e)$ is a negative-definite function [14]. It holds that:

$$\dot{V}(e) = 2e^T \dot{e} = 2e^T \frac{\mathrm{d}}{\mathrm{d}t}[\lambda_{sdq}^* - f_{dq}(i_{sdq})]$$
$$= -2e^T \boldsymbol{L} \frac{\mathrm{d}i_{sdq}}{\mathrm{d}t} = -2ke^T \boldsymbol{L} e \quad (8)$$

Being $\boldsymbol{L}$ a non-singular symmetric matrix, the application of the Rayleigh's inequality [14] yields:

$$\lambda_{\min}(\boldsymbol{L})\| e \|^2 \leq e^T \boldsymbol{L} e \leq \lambda_{\max}(\boldsymbol{L})\| e \|^2 \quad (9)$$

where $\lambda_{\min}(\cdot)$ and $\lambda_{\max}(\cdot)$ denote the minimum and maximum eigenvalues. Remind that all the eigenvalues of a symmetric matrix are real; moreover, a symmetric matrix is positive definite if and only if all its eigenvalues are positive. Hence, after combining (9) with (8), it follows that

$$\dot{V}(e) = 2ke^T \boldsymbol{L} e \leq -2k\lambda_{\min}(\boldsymbol{L})\| e \|^2 < \cdots < -2\,\mathrm{km}\| e \|^2 \quad (10)$$
$$< 0$$

where

$$m \overset{\Delta}{=} \min_{\boldsymbol{u} \in D} \lambda_{\min}(\boldsymbol{L}) \quad (11)$$

which proves the asymptotic stability of the closed-loop system for any choice of the integral gain $k > 0$ (note that m certainly exists because D is compact). The condition (10) can be used to derive an upper bound to the rate of convergence to zero of the regulation error norm $\| e \|$. By using definition (7), from (10) it follows that

$$\dot{V}(e) \leq -2\,\mathrm{km}V(e) \quad (12)$$

which in turns yield

$$V(e(t)) \leq V(e(0))\exp(-2kmt) \qquad (13)$$

or, equivalently

$$\| e(t) \| \leq \| e(0) \|\exp(-kmt) \qquad (14)$$

for $t \geq 0$. Therefore, from (14), it follows that the regulation error norm will certainly be less than a prescribed threshold e_T when

$$t > \frac{1}{km}\ln\left(\frac{\| e(0) \|}{e_T}\right) \qquad (15)$$

which represents an upper bound to the settling time of the regulation loop – indeed, the error can settle to zero faster than the upper bound specified in (14). Both the bounds (14) and (15) depend on the initial value $\| e(0) \|$ of the regulation error norm. By assuming that the initial state of the integrator (6) is zero, then the initial error norm $\| e(0) \|$ is upper bounded by

$$e_{0,\max} \underline{\triangleq} \max_{i_{dq} \in D} \| \boldsymbol{f}_{dq}(\boldsymbol{i}_{sdq}) - \boldsymbol{f}_{dq}(0) \| \qquad (16)$$

Note that it is always possible to assume that $\boldsymbol{f}_{dq}(\boldsymbol{0})$ is equal to zero (if not, as in the case of permanent-magnet motors, it is possible to remove it from the values stored in the LUTs of the map $\boldsymbol{f}_{dq}$, prior to the application the proposed method), so that

$$e_{0,\max} = \max_{i_{sdq} \in D} \| \boldsymbol{f}_{dq}(\boldsymbol{i}_{sdq}) \| = \max_{i_{sdq} \in D} \| \boldsymbol{\lambda}_{sdq}(\boldsymbol{i}_{sdq}) \| \qquad (17)$$

By using (17) within (15), the following upper bound to the settling time (to an error less than e_T) is obtained:

$$\bar{t}_s(e_T) = \frac{1}{km}\ln\left(\frac{e_{0,\max}}{e_T}\right) \qquad (18)$$

which is independent of the initial error norm $\| e(0) \|$.

The condition (18) can be used as a design equation: in fact, given the desired (maximum) settling time $\bar{t}_s(e_T)$ as a control performance specification, from (18) it is possible to determine the controller gain that allows the fulfilment of the specification, namely:

$$k = \frac{1}{m\bar{t}_s(e_T)}\ln\left(\frac{e_{0,\max}}{e_T}\right) \qquad (19)$$

Note that (19) requires to compute (11). For the 2×2 inductance matrix $\boldsymbol{L}$ in (2), with the additional reciprocity conditions (3), it is immediate to verify that

$$\lambda_{\min}(L) = \frac{(L_{dd} + L_{qq}) - \sqrt{(L_d - L_q)^2 + 4L_{dp}^2}}{2} \qquad (20)$$

so that (11) reduces to find the minimum of the function (20) over D.

5 Test on experimental data

The experimentally obtained LUTs representing the current-to-flux maps f_{dq} of an 11 kW SynRM are shown in Fig. 3, over the set $D = \{(i_{sd}, i_{sq}): |i_{sd}| \leq 20\,\text{A}, |i_{sq}| \leq 20\,\text{A}\}$. The differential inductances, obtained by numerical differentiation of the data in Fig. 3, are reported in Fig. 4.

For calculating f_{dq}^{-1}, assume that the required (maximum) settling time to 2% of the nominal flux linkage $\lambda_N = 0.57$ Vs is $\bar{t}_s(e_T) = 10$ ms (where $e_T = 0.02\ \lambda_N$). According to (18), the integrator gain that satisfies such specification is $k \simeq 88 \times 10^4$. With the proposed integral gain, the typical response of the normalised error norm $\| e(t) \|/\lambda_N$ is shown in Fig. 5, on both a linear and a logarithmic scale.

The figure is obtained by iterating the proposed method for each value stored in the LUT of the current-to-flux map f_{dq}, and then taking the slowest decaying response (dark solid line). The dashed line is the upper-bound to the normalised error norm, obtained by using (14) combined with (17).

It is noticed that the calculated upper bound is not very tight, and indeed the computed bound is roughly twice the actual maximum settling time. However, this condition is heavily dependent on the profile of the current-to-flux map, i.e. the machine under test. Different machines with different magnetic saturation characteristics may show the bound to be closer to the actual maximum settling time.

The final inverse flux-to-current map f_{dq}^{-1}, resulting after the application of the proposed method to each point of the LUTs in Fig. 3 is shown in Fig. 6. With an upper-bound to the settling time of 10 ms, the total time required for the calculation of the inverse map f_{dq}^{-1} on a 33×33 point grid over D is approximately equal to $33 \times 33 \times 10$ ms $\simeq 11$ s. This time can be obviously reduced by setting a smaller value of the settling time specification used to compute the integrator gain – such choice will simply produce a larger controller gain.

However, since the control scheme of Fig. 2 used for the map inversion is necessarily discrete in order to be simulated by a digital micro-controller (for example, by using the forward Euler method to approximate an integrator in the discrete time domain),
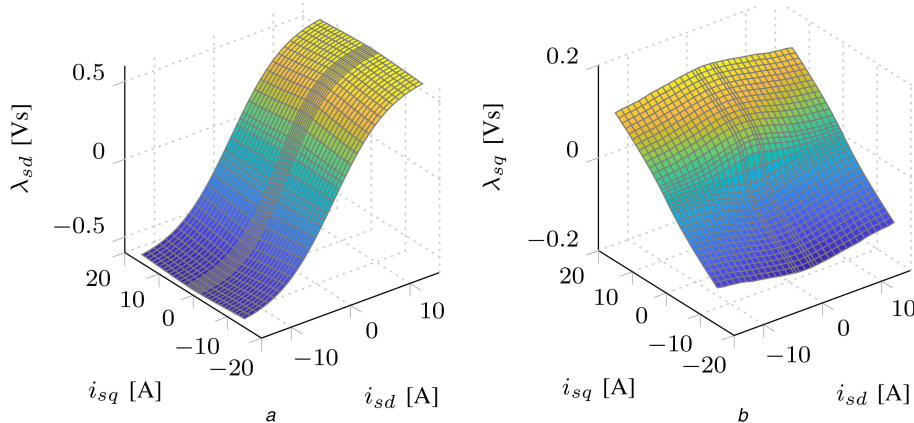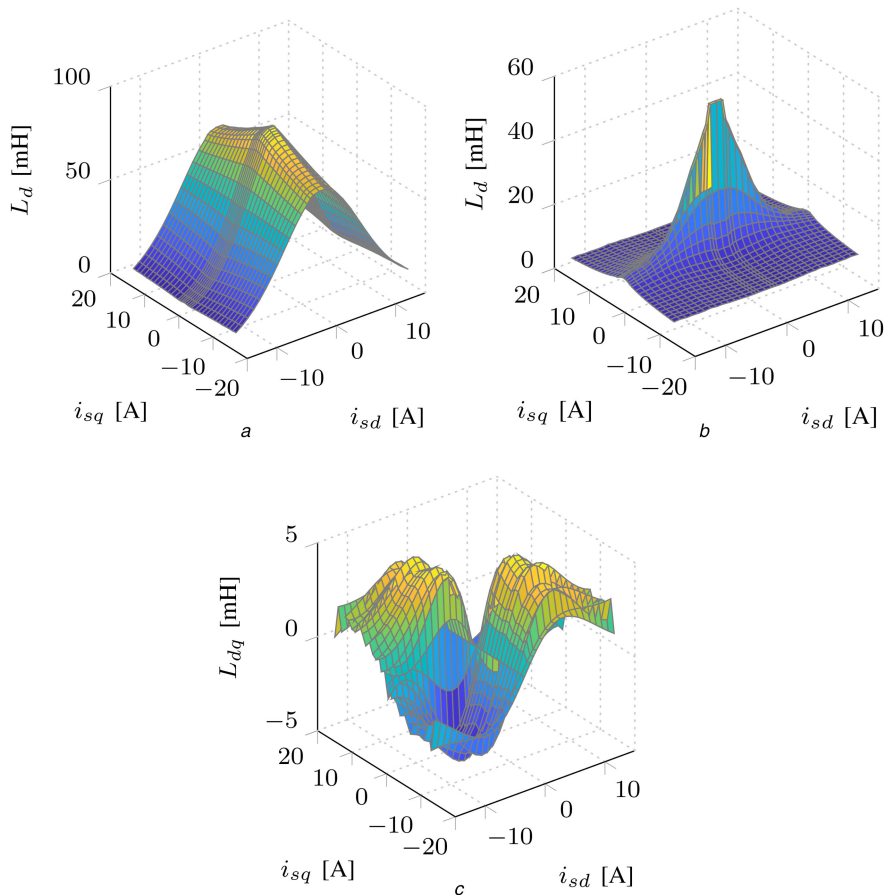

Fig. 3 *Current-to-flux maps*
(a) $\lambda_{sd} = f_d(i_{sd}, i_{sq})$, *(b)* $\lambda_{sq} = f_q(i_{sd}, i_{sq})$
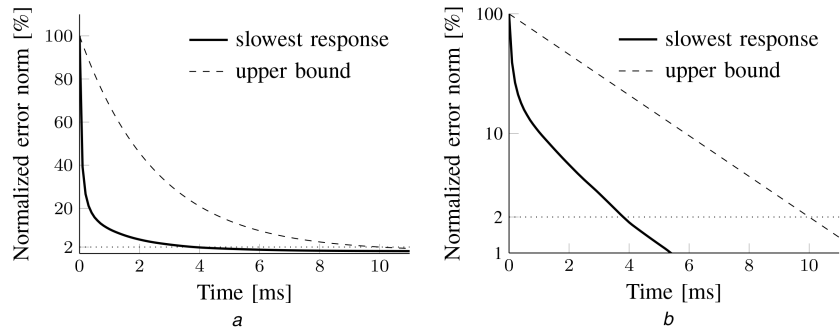
Fig. 5 *Convergence analysis*
(a) Linear scale plot, *(b)* Logarithmic scale plot
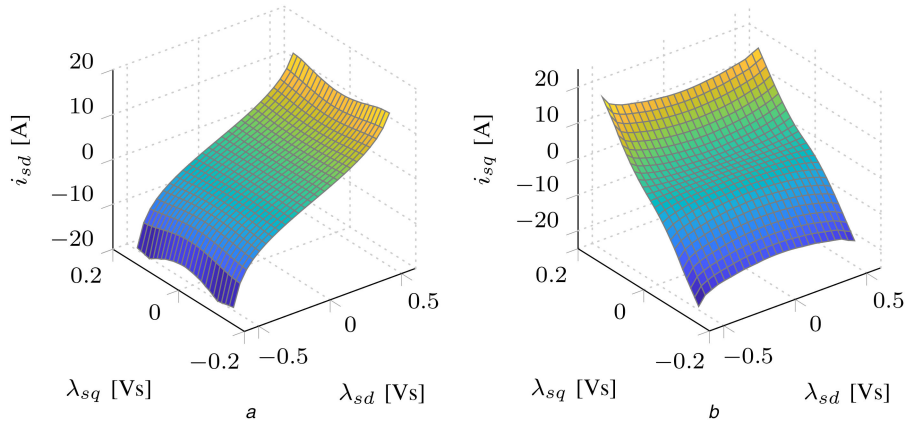
Fig. 6 *Flux-to-current maps*
(a) $i_{sd} = f_d^{-1}(\lambda_{sd}, \lambda_{sq})$, *(b)* $i_{sq} = f_q^{-1}(\lambda_{sd}, \lambda_{sq})$

Fig. 4 *Differential inductance maps*
(a) L_{dd}, *(b)* L_{qq}, *(c)* L_{dq}

there is obviously a lower bound on the selectable settling time specification, below which the discretisation becomes unstable. It is not easy to provide an analytic expression for the lower bound (it would be necessary to reformulate the entire analysis of Section 4 in the discrete time domain, which is a non-trivial task): from extensive simulations, it has been noted that stability is guaranteed whenever the required settling time is chosen larger than 50 sampling periods of the digital controller sampling time.

6 Conclusions

This paper discusses the calculation of the inverse magnetic saturation curves from flux linkages to currents in the *dq* reference frame, for their use in synchronous machine models where flux linkages are the state variables. After proposing a methodology that calculates the inverse curves based on a set of magnetic saturation curves from currents-to-flux linkages, the paper demonstrates its convergence, returning an upper bound limit for its settling time. This result allows the inclusion of the method in the commissioning of an electric drive, right after the estimation of the magnetic saturation curves.

The method has been tested on the experimentally measured magnetic saturation curves of a SynRM, proving its validity and that of the convergence analysis.

7 References

[1] Ali Awan, H.A., Tuovinen, T., Saarakkala, S., *et al.*: 'Discrete-time observer design for sensorless synchronous motor drives', *IEEE Trans. Ind. Appl.*, 2016, **52**, (5), pp. 3968–3979. Available at https://doi.org/10.1109/TIA.2016.2572105

[2] Tuovinen, T., Hinkkanen, M., Luomi, J.: 'Modeling of saturation due to main and leakage flux interaction in induction machines', *IEEE Trans. Ind. Appl.*, 2010, **46**, (3), pp. 3937–3945. Available at https://doi.org/10.1109/TIA.2010.2045210

[3] Mingardi, D., Morandin, M., Bolognani, S., *et al.*: 'On the proprieties of the differential cross-saturation inductance in synchronous machines', *IEEE Trans. Ind. Appl.*, 2017, **53**, (2), pp. 991–1000. Available at https://doi.org/10.1109/TIA.2016.2622220

[4] Vagati, A., Pastorelli, M., Scapino, F., *et al.*: 'Impact of cross saturation in synchronous reluctance motors of the transverse-laminated type', *IEEE Trans. Ind. Appl.*, 2000, **36**, (4), pp. 991–1000. Available at https://doi.org/10.1109/28.855958

[5] Mahmoud, H., Bianchi, N.: 'Nonlinear analytical model of eccentric synchronous reluctance machines considering the iron saturation and slotting effect', *IEEE Trans. Ind. Appl.*, vol. **53**, no. 3, pp. 2007–2015, 2017. Available at https://doi.org/10.1109/TIA.2017.2666085

[6] Li, Q., Fan, T., Wen, X.: 'Characterization of iron loss for integral-slot interior permanent magnet synchronous machine during flux weakening', *IEEE Trans. Magn.*, 2017, **53**, (5), p. 8101308. Available at https://doi.org/10.1109/TMAG.2017.2676094

[7] Zanuso, G., Peretti, L., Sandulescu, P.: 'Stator reference frame approach for DC injection-based stator resistance estimation in electric drives'. Proc. of the 11th IEEE Int. Conf. on Power Electronics and Drive Systems (PEDS), Sydney, Australia, 9–12 June 2015, pp. 867–872. Available at https://doi.org/10.1109/PEDS.2015.7203391

[8] Kim, Y.-S., Sul, S.-K.: 'Torque control strategy of an IPMSM considering the flux variation of the permanent magnet'. Conf. record of the 42nd IAS Annual Meeting, New Orleans, LA, USA, 23–27 September 2007, pp. 1301–1307. Available at https://doi.org/10.1109/07IAS.2007.202

[9] Peretti, L., Sandulescu, P., Zanuso, G.: 'Selfcommissioning of flux-linkage curves of synchronous reluctance machines in quasi-standstill condition', *IET Electr. Power Appl.*, 2015, **9**, (9), pp. 642–651. Available at https://doi.org/10.1049/ietepa.2015.0070

[10] Qu, Z., Tuovinen, T., Hinkkanen, M.: 'Inclusion of magnetic saturation in dynamic models of synchronous reluctance motors'. Proc. of the XX Int. Conf. on Electrical Machines (ICEM), Marseille, France, 2–5 September 2012, pp. 994–1000. Available at https://doi.org/10.1109/ICElMach.2012.6349997

[11] Urasaki, N., Senjyu, T., Uezato, K.: 'A novel calculation method for iron loss resistance suitable in modeling permanent-magnet synchronous motors', *IEEE Trans. Energy Convers.*, 2003, **18**, (1), pp. 41–47. Available at https://doi.org/10.1109/TEC.2002.808329

[12] Pairo, H., Shoulaie, A.: 'Effective and simplified method in maximum efficiency control of interior permanent magnet synchronous motors', *IET Electr. Power Appl.*, 2017, **11**, (3), pp. 447–459. Available at https://doi.org/10.1049/iet-epa.2016.0617

[13] Feynman, R.P., Leighton, R.B., Sands, M.L.: '*The feynman lectures on physics*' (1963, 2006, 2013). Available at http://www.feynmanlectures.caltech.edu/

[14] Khalil, H.K.: '*Nonlinear Systems*' (Prentice Hall, Upper Saddle River, NJ, USA, 2002, 3rd edn.), ISBN 0-13-067389-7. Available at http://www.egr.msu.edu/khalil/NonlinearSystems/